Phase-Matched Magnetization-Induced Second-Harmonic Generation in Yttrium–Iron–Garnet Magnetophotonic Crystals

Andrey A. Fedyanin, Oleg A. Aktsipetrov, Daisuke Kobayashi, Kazuhiro Nishimura, Hironaga Uchida, and Mitsuteru Inoue

***Abstract*—Magnetization-induced second-harmonic generation (MSHG) is studied in one-dimensional magnetophotonic crystals formed from a stack of ferromagnetic Bi-substituted yttrium–iron–garnet layers alternating with dielectric films. The resonance enhancement of reflected MSHG due to the phase-mismatch compensation is observed for longitudinal dc-magnetic-field application if the fundamental radiation is tuned across the photonic band gap edge. The high-contrast magnetization-induced variations in the second-harmonic intensity are obtained in transversal configuration of the nonlinear magnetooptical Kerr effect.**

***Index Terms*—Magnetooptic devices, magnetophotonic crystals, optical propagation in nonlinear media.**

ONE OF THE prospective applications of photonic crystals—the microstructures with the periodic modulation of the refractive index in one or several directions and possessing photonic band gap (PBG) [1], is their use for enhancement of the nonlinear-optical effects such as second-harmonic generation (SHG). The optical wave, which has the wave-vector component parallel to the periodicity direction nearby the PBG edge, possesses specific dispersion properties—anomalously small group velocity or the singularity in the photonic density of states [2]. This allows effective fulfillment of the phase-matching conditions for SHG in case as the fundamental or second-harmonic (SH) wave is tuned near the PBG edge. The use of one-dimensional (1D) photonic crystals—distributed Bragg reflectors, for the SHG phase matching has been proposed in [3]. Later on, the SHG enhancement at the PBG edge has been observed in Bragg reflectors formed from GaAs–AlGaAs [4], AlAs–AlGaAs [5], and ZnS–SrF_2 [6] layers, or alternating layers of porous silicon with different porosity [7]. Advantages of photonic crystals for applications can be expanded greatly by using magnetophotonic crystals (MPC), in which one or several layers of photonic crystal are formed from magnetic materials. MPC yield a mechanism for molding the flow of light flexible under external control impacts such as dc-magnetic field. MPC with the single magnetic layer squeezed between two high-finesse Bragg reflectors have been designed recently [8]. Such MPC act as magnetic photonic-crystal microcavities and have a resonant optical transition—microcavity mode, located in the PBG. Spatial localization of the optical wave resonant to the microcavity mode leads to the Faraday effect enhancement observed in MPC with the magnetic garnet [8] and Co-ferrite [9] spacers.

In magnetic noncentrosymmetric materials, the quadratic optical susceptibility tensor $\chi^{(2)}$ becomes a function of the magnetization vector $\mathbf{M}$. Nonlinear quadratic polarization contains two electric-dipole contributions. One of them is magnetization-induced term and leads to magnetization-induced second-harmonic generation (MSHG) [10]. Another term is independent on $\mathbf{M}$ and induces nonmagnetic SHG. Due to localization of the resonant fundamental radiation in the garnet spacer of MPC, the absolute values of both nonmagnetic and magnetization-induced SHG components are enhanced manyfold. This allowed the observation of the polar nonlinear magnetooptical Kerr effect in magnetophotonic crystals [11] manifested itself in magnetization-induced rotation of the SH wave polarization. In that case, MSHG came from the half-wavelength-thick magnetic spacer only. Enhancement of MSHG is expected also in MPC formed from numerous magnetic layers due to the phase-mismatch compensation at the PBG edge. However, the fabrication of Bragg reflectors with several magnetic layers remains the principle technological difficulty.

In this paper, the fabrication of magnetophotonic crystals formed from alternating layers of Bi-substituted yttrium–iron–garnet and silicon oxide is reported. The solely MSHG component of the SH field is detected in the longitudinal dc-magnetic-field application utilizing specific symmetry properties of the $\chi^{(2)}$ tensor. Its intensity is enhanced if the fundamental radiation is tuned across the PBG edge. The enhancement originates from the effective fulfillment of the phase matching conditions. The transversal nonlinear magnetooptical Kerr effect manifests itself in magnetization-induced variations of the SH intensity, which are odd in magnetization due to interference between magnetization-induced and nonmagnetic components of the SH wave.

MPC are fabricated from four repeats of $3\lambda_{\mathrm{MC}}/4$-thick layers of Bi-substituted yttrium–iron–garnet (Bi:YIG), $Bi_{1.0}Y_{2.0}Fe_5O_x$, and $\lambda_{\mathrm{MC}}/4$-thick SiO_2 layers, where λ_{MC} denotes the PBG center at the normal incidence. MPC with

Manuscript received October 15, 2003. This work was supported in part by a Grant-In-Aid from the Ministry of Education, Science, Culture and Sport of Japan (no. 14205045 and 14655119), the Russian Foundation for Basic Research (RFBR).

A. A. Fedyanin and O. A. Aktsipetrov are with the Department of Physics, Moscow State University, 119992 Moscow, Russia (e-mail: fedyanin@shg.ru; aksip@shg.ru).

D. Kobayashi, K. Nishimura, H. Uchida, and M. Inoue are with the Department of Electrical and Electronic Engineering, Toyohashi University of Technology, Toyohashi, Japan (e-mail: dkoba@maglab.eee.tut.ac.jp; uchida@eee.tut.ac.jp; nishimura@eee.tut.ac.jp; inoue_mitsuteru@eee.tut.ac.jp).

Digital Object Identifier 10.1109/TMAG.2004.832805

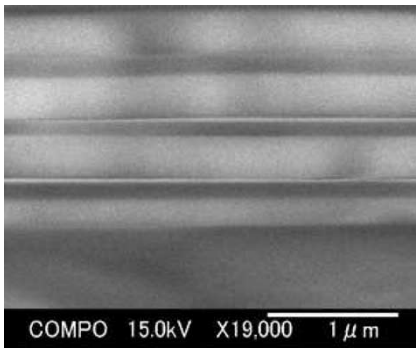

Fig. 1. FESEM image of the 1D-MPC with four Bi:YIG layers. Light strips correspond to magnetic garnet layers.

$\lambda_{\mathrm{MC}} \simeq 950$ nm are grown on a fused quartz substrate by RF sputtering of corresponding targets in the Ar^{+} atmosphere with pressure of 6 mTorr. After evaporation of each successive Bi:YIG layer, the sample is removed from sputtering chamber and annealed in air at 700 °C for 20 min for residual oxidation and crystallization of Bi:YIG film. The MPC cleavage image obtained in the field-emission scanning electron microscope (FESEM) is shown in Fig. 1. High lateral periodicity and sharp interfaces between magnetic garnet and dielectric layers are seen. Small gradual increase of the upper garnet layers thickness is apparently associated with different shrinkage of garnet films during annealing and changes in sputtering rate due to the change of substrate temperature during sputtering. Ferromagnetic properties of MPC are studied in vibrating sample magnetometer. Coercivity of MPC is approximately 30 Oe. Saturating magnetic field values slightly above 100 Oe indicate the easy-magnetization axis aligned in the MPC plane.

Optical transmission spectrum of MPC is shown in Fig. 2. Spectral region from 850 to 1100 nm with small transmission indicates the photonic band gap with the smallest transmission coefficient value of 0.12 reached at 965 nm. Outside the PBG, optical spectrum has the interference fringes, where transmission increases up to 0.9. The spectrum of the Faraday rotation angle θ_F measured in crossed Glan-prizm polarizer and analyzer with cooled photomultiplier tube is shown in Fig. 2 also. θ_F is enhanced up to $-0.8°$ at the long-wavelength edge of PBG at 1100 nm. It corresponds to $-0.75°/\mu$m, that is approximately eight times larger than the relative Faraday rotation angle for the single Bi:YIG film measured at this wavelength. Peaks of θ_F observed also at 750 and 830 nm correlate with the transmission spectrum maxima and ride on the monotonous θ_F increase with the wavelength decrease associated with Faraday rotation angle spectrum of Bi:YIG. Faraday rotation is strongly suppressed in the PBG.

The linear polarized output of a tunable ns-parametric generator/amplifier with wavelength λ_ω from 730 to 1150 nm is directed on the MPC at the 28° angle of incidence. The pulse duration is approximately 2 ns and energy is below 5 mJ/pulse. The SH radiation reflected from the MPC is selected by a series of glass filters and detected by a photomultiplier tube and a boxcar. The SH intensity spectrum is normalized on the intensity of the SH radiation reflected from the y-cut quartz plate taking into account the laser fluence and the spectral sensitivity of the optical detection system. The MSHG experiments are performed in the presence of the saturating dc-magnetic-field with the strength up to 2 kOe applied tangentially to the surface in transversal and longitudinal configurations using a permanent FeNdB magnet. The similar but weaker MSHG effects are expected in the absence of the external field due to remanence.

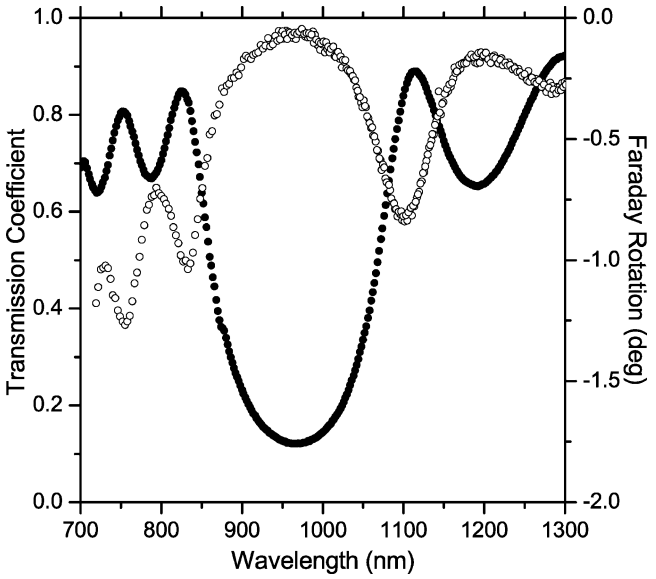

Fig. 2. Spectra of the transmittance (filled circles) and the Faraday rotation angle (open circles) of MPC with four Bi:YIG layers and $\lambda_{\mathrm{MC}} \simeq 950$ nm measured at the normal incidence.

MSHG arises from quadratic nonlinear polarization $\mathbf{P}_{2\omega}^{(2)}$ at the double frequency of the fundamental radiation $\mathbf{E}_\omega$, which is given in the electric-dipole approximation as $\mathbf{P}_{2\omega}^{(2)} = \chi^{(2)}(\mathbf{M}) : \mathbf{E}_\omega \mathbf{E}_\omega$. The dipole quadratic susceptibility tensor $\chi^{(2)}(\mathbf{M})$ can be expanded into the series over $\mathbf{M}$

$$\chi^{(2)} = \chi^{(2,0)} + \chi^{(2,1)} \cdot \mathbf{M} + \chi^{(2,2)} : \mathbf{MM} + \ldots. \quad (1)$$

Tensor $\chi^{(2,0)}$ describes the nonmagnetic crystallographic contribution to $\chi^{(2)}$, pseudotensor $\chi^{(2,1)}$ governs the magnetic contribution, which is odd in magnetization, and tensor $\chi^{(2,2)}$ is responsible for the magnetization-induced term even in $\mathbf{M}$. Since SiO_2 layers are centrosymmetric, dipole nonlinear sources are supposed to be localized in the magnetic Bi:YIG layers, which are considered as films isotropic in the surface plane. In the frame with the z axis being the film normal and xz being the plane of incidence, $\chi^{(2,0)}$ has three nonequivalent elements, χ_{zzz}, $\chi_{zxx} = \chi_{zyy}$, and $\chi_{xxz} = \chi_{yyz}$, while $\chi^{(2,1)}$ has six nonequivalent elements [12]: $\chi_{xzzY} = -\chi_{yzzX}$, $\chi_{zxzY} = -\chi_{zyzX}$, $\chi_{yxzZ} = -\chi_{xyzZ}$, $\chi_{yyyX} = -\chi_{xxxY}$, $\chi_{yxyY} = -\chi_{xxyX}$, $\chi_{xyyY} = -\chi_{yxxX}$, where the capital subscript corresponds to the $\mathbf{M}$ component.

The nonmagnetic (crystallographic) SH field $E_{2\omega}^{NM}$ induced by the $\chi^{(2,0)}$ tensor is equal to zero in the p-in, s-out polarization combination. Thus in longitudinal configuration, as $\mathbf{M} = (M_X, 0, 0)$, the SH intensity is entirely associated with the magnetization-induced SH field $E_{2\omega}^{M}$ induced by χ_{yxxX} and χ_{yzzX} components of the $\chi^{(2,1)}$ tensor. Fig. 3 shows the spectrum of the SH intensity measured in the p-in, s-out polarization combination. Spectrum demonstrates the resonant enhancement at $\lambda_\omega \simeq 1055$ nm. The spectral position of the peak correlates

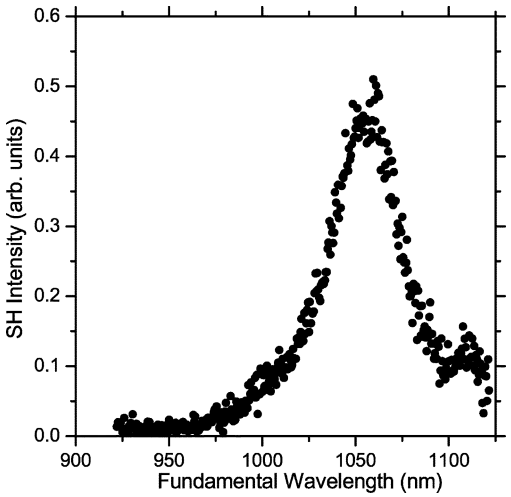

Fig. 3. Intensity spectrum of the SH wave reflected from MPC in the p-in, s-out polarization combination and in longitudinal configuration of the dc-magnetic field application.

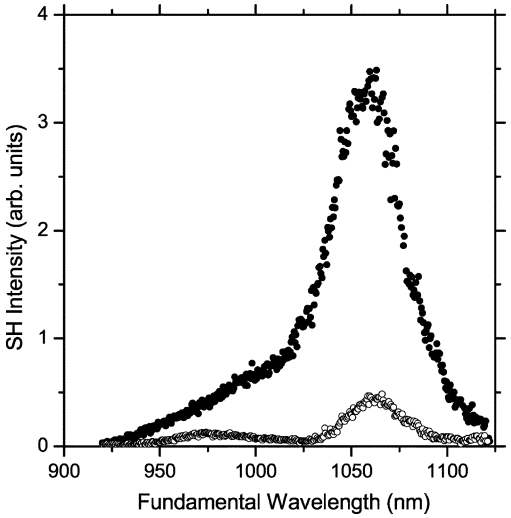

Fig. 4. SHG spectra of MPC in the p-in, p-out polarization combination and in transversal magnetic-field configuration measured for opposite directions of the dc-magnetic field, open and filled circles, respectively.

with the long-wavelength PBG edge, which is blue-shifted due to oblique angles of incidence. The MSHG enhancement is interpreted as a result of the phase matching at the PBG edge. Inverting the magnetic field direction does not change the value of the SH intensity that also proves the absence of the $E_{2\omega}^{NM}$ field. This is in contrast to the p-in, p-out polarization combination. In transversal configuration, as $\mathbf{M} = (0, M_Y, 0)$, the nonmagnetic SH field $E_{2\omega}^{NM}$, which is induced by χ_{zzz}, χ_{zxx}, and χ_{xxz} elements of the $\chi^{(2,0)}$ tensor, interferes with the magnetization-induced SH field $E_{2\omega}^{M} \exp(i\varphi_M)$ generated by χ_{xzzY}, χ_{zxzY}, and χ_{xxxY} components of the $\chi^{(2,1)}$ pseudotensor. The SH intensity contains the cross-term $\pm 2E_{2\omega}^{NM} E_{2\omega}^{M} \cos\varphi_M$ changing the sign upon inverting the magnetic field direction. This term shows the internal homodyne effect in MSHG and leads to variations of the SH intensity, which are linear in $\mathbf{M}$ and depends on the relative phase φ_M between $E_{2\omega}^{NM}$ and $E_{2\omega}^{M}$. Fig. 4 shows the SHG spectra measured for two directions of saturated magnetic field in transversal configuration. The SH intensity is enhanced manyfold in the vicinity of 1050 nm corresponding to the phase-matched conditions for SHG at the long-wavelength PBG edge of MPC. Inverting the magnetic field direction varies the SH intensity approximately by a factor of seven at $\lambda_\omega \simeq 1055$ nm that indicates the noticeable interference between the $E_{2\omega}^{NM}$ and $E_{2\omega}^{M}$ fields. At $\lambda_\omega \simeq 1025$ nm the SH intensity for one of the magnetic field direction is close to zero. It means that the contrast of the magnetization-induced variations in the SH intensity is close to unit, which the upper limit for the SHG magnetic contrast.

In conclusion, magnetization-induced second-harmonic generation reveals the intensity enhancement by a factor of more than 10^2 if the fundamental radiation is tuned across the photonic band gap edge of 1D magnetophotonic crystals consisted of stack of magnetic garnet layers. The enhancement is a manifestation of the phase matching for MSHG fulfilled at the PBG edge of magnetophotonic crystals.

REFERENCES

[1] K. Sakoda, *Optical Properties of Photonic Crystals*. Berlin, Germany: Springer-Verlag, 2001, p. 353.

[2] M. Scalora, M. J. Bloemer, A. S. Manka, J. P. Dowling, C. M. Bowden, R. Viswanathan, and J. W. Haus, "Pulsed second-harmonic generation in nonlinear, one-dimensional, periodic structures," *Phys. Rev. A*, vol. 56, pp. 3166–3174, 1997.

[3] N. Bloembergen and A. J. Sievers, "Nonlinear optical properties of periodic laminar structures," *Appl. Phys. Lett.*, vol. 17, pp. 483–485, 1970.

[4] J. van der Ziel and M. Ilegems, "Optical second harmonic generation in periodic multilayer GaAs–$Al_{0.3}Ga_{0.7}$–As structures," *Appl. Phys. Lett.*, vol. 28, pp. 437–439, 1976.

[5] Y. Dumeige, P. Vidakovic, S. Sauvage, I. Sagnes, J. A. Levenson, C. Sibilia, M. Centini, G. D'Aguanno, and M. Scalora, "Enhancement of second-harmonic generation in one-dimensional semiconductor photonic band gap," *Appl. Phys. Lett.*, vol. 78, pp. 3021–3023, 2001.

[6] A. V. Balakin, V. A. Bushuev, N. I. Koroteev, B. I. Mantsyzov, I. A. Ozheredov, A. P. Shkurinov, D. Boucher, and P. Masselin, "Enhancement of second-harmonic generation with femtosecond laser pulses near the photonic band edge for different polarizations of incident light," *Opt. Lett.*, vol. 24, pp. 793–795, 1999.

[7] T. V. Dolgova, A. I. Maidykovski, M. G. Martemyanov, A. A. Fedyanin, O. A. Aktsipetrov, G. Marowsky, V. A. Yakovlev, and G. Mattei, "Giant microcavity enhancement of second-harmonic generation in all-silicon photonic crystals," *Appl. Phys. Lett.*, vol. 81, pp. 2725–2727, 2002.

[8] M. Inoue, K. Arai, T. Fujii, and M. Abe, "One-dimensional magnetophotonic crystals," *J. Appl. Phys.*, vol. 85, pp. 5768–5770, 1999.

[9] E. Takeda, N. Todoroki, Y. Kitamoto, M. Abe, M. Inoue, T. Fujii, and K. Arai, "Faraday effect enhancement in Co-ferrite layer incorporated into one-dimensional photonic crystals working as a Fabry-Pérot type resonator," *J. Appl. Phys.*, vol. 87, pp. 6782–6784, 2000.

[10] R.-P. Pan, H. Wei, and Y. Shen, "Optical second-harmonic generation from magnetized surfaces," *Phys. Rev. B*, vol. 39, pp. 1229–1234, 1989.

[11] A. Fedyanin, T. Yoshida, K. Nishimura, G. Marowsky, M. Inoue, and O. A. Aktsipetrov, "Magnetization-induced second-harmonic generation in magnetophotonic microcavities based on ferrite garnets," *JETP Lett.*, vol. 76, pp. 527–531, 2002.

[12] A. V. Petukhov, I. L. Lyubchanskii, and T. Rasing, "Theory of nonlinear magneto-optical imaging of magnetic domains and domain walls," *Phys. Rev. B*, vol. 56, pp. 2680–2687, 1997.